A Population Based Ultra-Widefield Digital Image Grading Study for AMD-like Lesions at the Peripheral Retina

Imre Lengyel PhD[1], Adrienne Csutak MD PhD[2,5], Daniela Florea PhD[1,2], Irene Leung BA[2], Alan C Bird MD[1], Fridbert Jonasson MD[4] and Tunde Peto MD PhD[2]

[1]UCL Institute of Ophthalmology, University College London, London, England; [2]NIHR Biomedical Research Centre, at Moorfields Eye Hospital NHS Foundation Trust and UCL Institute of Ophthalmology, London, England; [4]Faculty of Medicine University of Iceland, Reykjavik, Iceland; [5]University of Debrecen, Faculty of Medicine, Department of Ophthalmology, Debrecen, Hungary

Running head: Ultra-widefield imaging of AMD-like lesions

Address for reprints:
Tunde Peto MD, PhD
Reading Centre, Department of Research and Development
Moorfields Eye Hospital NHS Foundation Trust
162 City Road, London, EC1V 2PD, UK
email: Tunde.Peto@moorfields.nhs.uk

Purpose: Our understanding of the relevance of peripheral retinal abnormalities to disease in general and in age-related macular degeneration (AMD) in particular is limited by the lack of detailed peripheral imaging studies. The purpose of this study was to develop image grading protocols suited to ultra-widefield imaging (UWFI) in an aged population.

Design: A cross-sectional study of a random population sample. The UWFI modality was introduced at the 12 year review of the Reykjavik Eye Study in Iceland.

Participants: 576 subjects aged 62 years or older participated in this study.

Methods: Ultra widefield (up to 200°) color and autofluorescence (AF) images were taken using the Optos P200CAF laser scanning ophthalmoscope. The images were graded at Moorfields Eye Hospital Reading Centre primarily based on the International Classification for AMD. Macular and peripheral changes were graded using a standardised grid developed for this imaging modality.

Main Outcome Measures: Presence or absence of hard, crystalline and soft drusen, retinal pigment epithelial changes, choroidal neovascularization (CNV), atrophy and hypo- and hyperautofluorescence were graded in the peripheral retina.

Results: 81.1% of the eyes examined had AMD–like changes; in the macula alone (13.6%), periphery alone (10.1%) and both periphery and macula (57.4%). There was no AMD-like CNV or pigment epithelial detachment (PED) in the periphery except in those cases in which these clearly originated from the macula. Seven patients had AMD-like atrophy in the periphery without end-stage disease in the macula. One patient with end-stage disease in the macula had a normal periphery on the color images. While analyzing the eyes we detected pathological appearances that were very reliably identified by graders.

Conclusions: Phenotyping the retinal periphery using the categories defined by the International Classification confirmed the presence of wide ranging AMD-like pathological changes even in those without central sight threatening macular disease.

63   Based on our observations we propose here new, reliably identifiable grading

64   categories that might be more suited for population based UWFI.

65

66   **Keywords:** age-related macular degeneration, image grading, geographic atrophy,

67   choroidal neovascularization, drusen, imaging, autofluorescence

68

69   Early and late age-related macular degeneration (AMD) show distinct topographical

70   patterns of change in the outer retina. Whilst the diagnosis relies on changes in the

71   macula, there are many age-related changes in the peripheral fundus [1, 2] that may be

72   associated with certain sub-types of AMD such that recording peripheral changes may

73   be important in generating more accurate AMD phenotypes which could then guide

74   treatment strategies. Wide field imaging protocols such as the five or seven field

75   images were generated in the past[3, 4] but most publications are for diabetic retinopathy,

76   not for AMD. These imaging protocols allowed the visualization of approximately 75°

77   fields. Ultra-widefield imaging (UWFI) of the retina of up to 200° is now available

78   through the use of Optos P200CAF, a scanning laser ophthalmoscope (Optos plc,

79   Scotland, UK). Conventional and UWFI grading in the macula showed excellent

80   correlation [5], therefore the P200CAF can be used to detect reliably central changes

81   such as drusen, pigmentary changes, choroidal neovascularization (CNV) and

82   geographic atrophy (GA) implying that this imaging modality could be used for grading

83   for changes outside the macular region. Here we present grading protocols and the

84   results of UWFI of patients participating in the 12 years review of the Reykjavik Eye

85   Study. As far as we know this is the first time UWFI was employed in a population

86   based study for AMD-like changes that analyses color as well as autofluorescent

87   peripheral images.

88

89

90 **<u>Methods</u>**

91 The Reykjavik Eye study includes a random sample from the Reykjavik population

92 census of 50 years and older in 1996, in which 1045 person participated, all had an eye

93 examination and stereo fundus photography using films. [6] In 2008 the 12-year review

94 was conducted in which 576 persons participated, representing 73% of the survivors.

95 Participants of this review were photographed using the P200CAF, an ultra-widefield

96 (200˚) scanning laser ophthalmoscope that was operated by an Imaging Team

97 provided by Optos plc and supervised by the Reading Centre of Moorfields Eye

98 Hospital (MEHRC). In general, imaging with the Optos P200CAF does not require

99 dilation, though through the patients' involvement in other examinations in the

100 Reykjavik Eye Study their pupils were all dilated using Mydriacyl 1% (Alcon) and

101 Phenylephrine hydrochloride 10% (Akron). The P200CAF uses red (633 nm) and green

102 (532 nm) lasers to generate color images which are reflected off a large concave

103 elliptical mirror. The resulting images are displayed as red only, green only and a

104 combined red–green "false color" images. The area to grade on an UWFI is

105 significantly larger than the area covered by "classical" fundus image (Fig.1 A). The

106 P200CAF is also capable of taking autofluorescent images by using the green (532

107 nm) laser for excitation and record the autofluorescent emitted signal by a bright-band

108 detector (570 to 780 nm) (Figure 1 D,F,H). Each image had a resolution of 3000 by

109 3000 pixels.

110 Tenets of the Declaration of Helsinki were followed. Ethical approvals were obtained

111 from the Icelandic Data Protection Authority and the Icelandic National Bioethics

112 Committee. Signed informed consent was obtained from each participant. The digital

113 images were sent to the MEHRC with a unique ID number displayed on all

114 photographs. These ID numbers were used to identify patients and grading records in

115 the Reykjavik Eye Study.

116 Images were graded without access to clinical information using the Optos V2 vantage

117 DX review software provided with the camera. Using this software the grader was

118 allowed to modify gamma on the images, no other modification was allowed. The

119 review software was modified to allow the automatic fitting of an ultra-widefield grid that

120 (Fig.1 B) was based on the original definition of a standard macular grid (Zone1-3).

121 Concentric rings were defined based on the distance between the centers of the optic

122 nerve head and the foveola (defined to be 4,500 μm) using the pre-specified macular

123 grid of the International Classification and the Age-Related Eye Disease Study.[7, 8] This

124 definition was necessary to be able to compare zones 1-3 on UWFI and conventional

125 45º images. Macular comparison showed no substantial differences in disease severity

126 as reported earlier.[5] In addition to the macular zones, two further zones were created,

127 Zone 4 for the mid-periphery (with a diameter of 11,000 μm) and Zone 5 for the far

128 periphery, essentially all areas outside Zone 4 (Fig 1 B). These zones were generated

129 on un-projected (without correction for possible peripheral distortion) images, as this

130 function was not available at the time of the grading. It is also important to note that

131 there was no precedent of grading peripheral retinal UWFI changes at the time of this

132 grading and therefore these zones (Fig.1 B; Zones 4 and 5) were arbitrary. The zones

133 were subdivided into 4 quadrants through the center of the fovea (Fig. 1 B), creating

134 temporal and nasal superior, and temporal and nasal inferior quadrants. Only

135 abnormalities resembling early and late AMD were graded. Detailed grading was

136 conducted on all images by the same person using the categories of the International

137 Classification[7] in all quadrants and Zones: hard, crystalline and soft drusen, retinal

138 pigment epithelial changes, pigment epithelial detachment (PED), atrophy and CNV

139 were graded. On AF images hyper- and hypoautofluorescence (HyperAF and HypoAF,

140 respectively) changes were recorded. Incidental findings were commented on the

141   grading form. As this was a novel imaging modality, there was no grading scheme and

142   trained grader available. Therefore, extensive training and validation of the detailed

143   grading protocol took place before the grader for this study was certified. As such there

144   was no inter-grader variability calculated for the detailed grading. Intra-observer

145   agreement was calculated once 20%, randomly selected, images were re-graded after

146   14 days by the same certified grader and exact agreement and kappa statistics were

147   calculated. A new, simplified grading protocol, based on the overall assessment of the

148   entire color images, was developed after the detailed grading by the Authors. Two

149   graders were trained to use this simplified grading protocol and this time inter-grader

150   variability was also calculated. Kappa statistics was used to determine concordance

151   between appearance of changes between zones and quadrants and symmetry

152   between the two eyes. The Kappa (κ) statistic was interpreted as follows: κ <0 no

153   agreement; κ values 0-0.2 "slight", 0.21-0.40 "fair", 0.41-0.60 "moderate", 0.61-0.8

154   "substantial" and κ >0.81 "almost perfect agreement".[10] Statistical analysis was

155   performed using Stata 9.0 (STATA Data analysis & Statistical Software, Texas, USA).

156

157 **Results**

158 **Comparison of macular and peripheral abnormalities:**

159 *Color images:* At the 12 year review the 576 participants examined were 62 years or

160 older. Median age was 72 years. Main reasons for the loss of participants were death

161 during the 12 years since the baseline study, accounting for 42.1% among those 50-59

162 years at baseline and 77.3% among those 70-79 years at baseline. Other reasons

163 included frailty and immobility: 16% of among those 50-59 years at baseline to 28.1%

164 among those 70-79 years at baseline, despite offering free transport to the clinic. Sex

165 distribution among those attending and that not attending was similar. Of the total of

166 1,152 (576 participants) eyes, 14 (7 participants) (1.2%) could not be imaged by Optos

167 P200CAF due to fatigue (this imaging modality was Station 10 of the 11 station study)

168 or inability to open eyes. The UWFI of the remaining 1,138 (569 participants) eyes

169 were sufficiently good quality for grading.

170 Based on a simplified clinical grading that assessed only the presence or absence of

171 abnormalities, two hundred fifteen eyes (18.9%) had no observable abnormality either

172 in the macula (Zone 1-3) or periphery (Zone 4 and 5) and 653 (57.4%) had

173 abnormalities at both locations (Table 1 A). Lesions in the macula only were present in

174 155 (13.6%), and in the periphery was present only in 115 (10.1%) eyes (Table 1 A).

175 The concordance between clinical grading in the left and the right eyes were moderate

176 for both the macula ($\kappa=0.57$, $p<0.001$) and the periphery ($\kappa=0.45$, $p<0.001$). The

177 concordances in clinical grading between macula vs. periphery within the same eye

178 were fair for both right ($\kappa=0.39$ $p<0.001$) and left ($\kappa=0.32$, $p<0.001$) eyes. This grading

179 protocol was devised by the authors, one of whom was trained as a grader. Ten

180 percent of the images were reviewed by the clinical lead following random selection

181 generated by an independent third party statistician with no access to the grading data

182 or to the images. Given that we only had one trained grader, only intra-grader reliability

183 was undertaken. Intra-grader reliability was high in all categories ($\kappa >0.81$, $p<0.001$).

184   Temporal drift grading was not undertaken as all image analysis was finalized within 4

185   months.

186   Table 2 shows the cross tabulation of the macular and peripheral phenotypes. No

187   clearly definable PED could be seen in the periphery. Of the 155 eyes that were graded

188   as normal in the periphery, 154 had drusen and one had a mixed phenotype (both CNV

189   and GA were present in the macula and it was not possible to decide the nature of the

190   original lesion). Of those that were normal in the macula, 9 had retinal pigment

191   epithelial changes, 105 drusen and 1outer retinal atrophy at the periphery. Almost half

192   of the eyes had drusen both in the macula and in the periphery (560; 49.2%). Those

193   with end stage disease in the macula (34) all except one had visible lesions in the

194   periphery. CNV in the macula (13) was associated with drusen or mixed CNV and

195   atrophy at the periphery, but no CNV-only case was seen in the periphery. Of the 12

196   GA cases in the macula, 8 had drusen only and 4 had atrophy in the periphery.

197   Macular PED was associated with drusen only in the periphery, while the 7 eyes with

198   mixed macular phenotype (CNV and GA together) were associated with no visible

199   changes in 1, drusen only in 5 and atrophy in 1 eye.

200

201   *AF images:* Of the 576 participants UWF AF images were also acquired. Of the total of

202   1,152 AF images 28 images (2.4%) were considered missing due to the participant's

203   inability to tolerate a second imaging due to fatigue or inability to open eyes. The UWFI

204   of the remaining 1,124 eyes were sufficiently good quality for grading for AF in the

205   periphery. Overall 39 eyes had lesions in the macula (laser burns, disciform scar, or

206   branch retinal vein occlusion on color images) that made AF grading inconclusive.

207   These were excluded from the analysis.

208   Based on a simplified grading scheme termed here as clinical grading that assessed

209   the presence or absence of AF abnormalities 738 eyes (67.7%) had no observable

210   abnormality either in the macula (Zone 1-3) or periphery (Zone 4 and 5) and 81 (7.4%)

211 had abnormalities at both locations (Table 1 B). AF abnormality in the macula only was

212 present in 70 (6.4%), and in the periphery only was present in 201 (18.4%) eyes (Table

213 1 B).

214 The concordance between clinical AF grading in the left and the right eyes was

215 moderate for both the macula (κ=0.61, p<0.001) and the periphery (κ=0.48, p<0.001).

216 The concordance in clinical AF grading between macula vs. periphery within the same

217 eye were fair for both right (κ=0.25 p<0.001) and left (κ=0.22, p<0.001) eyes. Intra-

218 grader reliability was high in all categories (κ >0.81, p<0.001).

219

220 **Detailed peripheral grading:**

221 For further analysis, Zones 4 and 5 were subdivided into 4 quadrants for better

222 definition of the spatial distribution of abnormalities (Figure 2; details are in

223 Supplementary Table 1, available at http//aaojournal.org). Based on size on the

224 unprojected images drusen were either hard (<125 um), soft (>125 um) or crystalline.

225 Hard drusen were distributed across the retinal periphery but were most common in the

226 superior-nasal quadrant in Zone 5. The least hard drusen were seen in the inferior-

227 temporal quadrant. Soft drusen were most common in the superior quadrants with

228 similar level of deposition in both Zone 4 and Zone 5 here. Retinal pigment epithelial

229 changes were found mainly in Zone 5 with a trend for the superior quadrants. Both

230 hypo- and hyperautofluorescent changes were observed in higher prevalence nasally

231 than temporally especially in Zone 5. For crystalline drusen, choroidal

232 neovascularization and atrophy the numbers are too small to draw conclusions about

233 distribution.

234 The symmetry of changes between different categories and quadrants in the left and

235 right eyes ranged between fair to substantial. The most consistent symmetry was

236 detected for atrophy in all quadrants of Zone 5 (κ: 0.72-0.75, p<0.001) with wider

237 variability in zone 4 (κ: 0.39-0.80, p<0.001). The symmetry for hard drusen was

238 moderate (κ: 0.46-0.58, p<0.001) in Zone 4 and fair to moderate in Zone 5 (κ: 0.25-

239 0.52, p<0.001). In the case of soft drusen the symmetry was fair (κ: 0.32-0.45,

240 p<0.001) for all quadrants and zones. Pigmentary changes showed fair symmetry in

241 zone 4 (κ: 0.22-0.30, p<0.001) and moderate symmetry in zone 5 (κ: 0.50-0.64,

242 p<0.001). Symmetry for hypoautofluorescence was moderate (κ: 0.36-0.63, p<0.001)

243 and for hyperautofluorescence fair to moderate (κ: 0.16-0.47, p<0.001) for all

244 quadrants and zones. Numbers for other abnormalities were too low to obtain valid

245 comparisons.

246 Based on the grading data, it appears that the supra nasal quadrant is the most

247 affected in this patient population (Fig.2). Therefore, we determined the possible

248 correlation between the appearance of an abnormality in the supra nasal quadrant with

249 the same abnormality in the other quadrants within Zone 4 or Zone 5. The best

250 correlation was found between SN and IN for all categories (κ: 0.66-0.87, p<0.001)

251 except for soft drusen where the best correlation was between SN and ST (κ: 0.48-

252 0.78, p<0.001) supporting the findings on Figure 2 (and Supplementary Table 1,

253 available at http//aaojournal.org).

254 Next we determined whether the appearance of a certain lesion in SN Zones 4 or 5 is

255 associated with the appearance of any another type of lesion in the same quadrant. We

256 found mainly fair correlation between most categories (κ: 0.21-0.40, p<0.001). The only

257 exception was the almost perfect correlation between hypo- and

258 hyperautofluorescence in Zone 4 (κ=0.82, p<0.001). The correlation between the

259 appearance of a lesion in Zone 4 and 5 showed a fair correlation (κ: 0.21-0.40,

260 p<0.001) except for soft drusen where there appears to be a moderate correlation

261 (κ=0.53, p<0.001) and for atrophy where the correlation is poor (κ<0, p<0.001).

262 *Novel grading categories*

263 Following the detailed grading above, specific phenotypic patterns emerged that could

264 not be assigned to the previously described quadrants and zones (Fig. 3). We found

265   that 10.6% of all eyes contained large fields of peripheral hard drusen (it is labelled as

266   PHDF on Fig. 3 A and B). The most prevalent peripheral lesion we termed as

267   peripheral reticular degeneration, with its characteristic pigmentary changes (labelled

268   as PRD on Fig. 3 G and H) that was associated with 18.3% of the eyes. Drusen

269   deposition located next to the arcade vessels were present in 5.7% (labelled as AD on

270   Fig. 3 E and F) and peripheral soft drusen field was present in 2.5% of the eyes

271   (labelled as PSD on Fig.3 C and D). Overall 28.5% of the eyes had at least one and

272   7.7% had more than one of the new peripheral grading categories. The most important

273   observation with these grading categories was that there was no significant

274   disagreement between two independent observers (kappa>0.95; p<0.05 for all

275   categories).

276

Discussion

278 Ultra-widefield images had not previously been used to grade population based

279 peripheral retinal changes associated with early or late AMD although the presence of

280 pathological abnormalities up to the *ora serrata* had been well described.[11, 12] Here we

281 graded UWFI based on the International Classification[7] and report AMD-like

282 abnormalities in the periphery on both color and autofluorescent images. These

283 changes are associated with specific geographic location. During detailed grading it

284 emerged that there are patterns of abnormalities that do not rely on zones and

285 quadrants and highly reproducible in grading and could be used for grading for

286 peripheral retinal phenotyps.

287 Comparison of grading of macular abnormalities on images obtained with the Optos

288 P200CAF with non-stereoscopic conventional digital fundus images (45˚) showed no

289 substantial differences between grading for AMD in the macula.[5] These Optos

290 P200CAF images were gradable in the macula even on images that fell short of

291 grading standards on conventional fundus images [5]. This was due to the capacity of

292 laser beams to overcome problems with media opacities [13, 14] and have higher

293 resolution in terms of sharpness and contrast [15] than conventional color images. Due to

294 these factors, only 1.2% of the patients could not be imaged in this study and that was

295 due to non-compliance and not difficulty with the imaging itself. This built confidence in

296 using UWFI for grading AMD-like changes outside of the macula.

297 Throughout the grading of the peripheral retina there were several issues that needed

298 to be addressed. Graders had to learn to appreciate artifacts related to the broad depth

299 of focus of this device such as the presence of eyelids, eyelashes, floaters, the optics

300 and the haptics of the intraocular lens or lens opacities and the fact that the images, as

301 they are generated by green and red laser lights rather than the more widely used

302   white light illumination, are less familiar to graders in the first instance (examples are

303   shown on Fig. 1 and 3). Occasionally grading of more than one image had to be carried

304   out on the same eye due to blinking or difficulty to open the eye lids. The reported

305   distortion at the peripheral retina [18] had also posed issues in how this might affect the

306   perceived size of drusen and the grading of quadrants especially in Zone 5. However,

307   we found that most of these aspects can be overcome or minimized with practice and

308   good imaging techniques and felt that distortions are unlikely to affect the overall

309   conclusions of this study. How, if at all, previously reported problems with the Optos

310   P200, an earlier device, in misdiagnosis and artefacts related to broad depth of field[16,

311   17] might affect far peripheral grading for early and late AMD using Optos P200CAF

312   images will need to be evaluated in follow-up studies.

313   Using flat mount cadaveric eyes it has been shown that pathological changes external

314   to the RPE are often "masked" by the presence of the RPE.[11] Therefore, the peripheral

315   retina changes seen in this UWFI study are likely to be underestimates. Whether or not

316   these hidden changes become clinically evident with time need to be evaluated in

317   follow-up studies. Masking effects in the superior and inferior periphery by the eyelids,

318   and eyelashes and loss of image quality may add to this underestimation. The loss of

319   imaging fields was variable between participants (Figure 1), but had not been

320   estimated here. Some of the loss could potentially be overcome by generating steered

321   images. This, however, was not attempted in this study due to the need to image large

322   volume of patients (~100 participants in a day) and the time constrains due to UWFI

323   being only one of the 11 examination st ations in this study. By overcoming the

324   problems associated with loss of field and correcting for the warping of images, new

325   UWF ophthalmoscopes will lead to a more streamlined, more accurate and faster

326   imaging of AMD-like abnormalities at the peripheral retina in large populations.

327   The fact that the majority of affected eyes had changes at both the macula and the

328   periphery shows that the abnormalities leading to AMD may not only be restricted to

329   the macula. To understand the significance of peripheral retina changes to disease

330   progression, it will be necessary to review these patients from time to time. The

331   observation that there are eyes with only macular or only peripheral changes (Table 1),

332   reflects the diversity of AMD-like changes that is likely to be related to the various risk

333   factors.

334   Overall, we can confidently say that in the Reykjavik eye study population peripheral,

335   especially far peripheral, drusen deposition, pigmentary changes, hypo and hyper AF

336   changes are abundant in most eyes. However, the number of eyes with crystalline

337   drusen, CNV or atrophy were too few to ascertain the spatial distribution of these

338   categories with confidence. The intriguing finding that pathological changes show

339   specific special distributions (Figure 2) will require further investigations. For example,

340   it will be interesting to learn why there were more numerous hard drusen deposited

341   nasally with a preference for the superior quadrant (Figure 2) and why soft drusen were

342   enriched in the superior quadrants (Figure 2). The relationships between the

343   appearance of abnormalities in zone 4 and zone 5 are not strong (kappa <0.60)

344   suggesting that their development at these different eccentricities are probably not

345   closely related and this gives support to our choice of subdivision of the peripheral

346   retina (Figure 1, B). Overall, lesions were most prevalent in zone 5 (Figure 2), an area

347   known to be prone to ophthalmoscopic abnormalities throughout life. What anatomical

348   features determine the regional distribution of changes in the periphery is unknown.

349   One potential contributor might be the nature of the choroidal vasculature and the

350   associated metabolic supply.[19, 20]

351   It is intriguing that the superior nasal quadrant is most prone to pathological changes in

352   this population. One explanation might be related to photo oxidative damage triggered

353   by solar UV-radiation that arrives from a lower zenith angle in Iceland than most other

354   countries. The lower zenith angle had been associated with an increased risk for

355   cortical cataract development in the superior quadrant in this population.[21] Therefore,

356   UWFI of other aged populations will be needed to evaluate whether the same

357   predilection is true in other communities.

358   While detailed grading revealed some intriguing special differences, this grading might

359   not be easy to implement in a clinical environment. However, during the original

360   grading of these eyes, several characteristic patterns emerged (Figure 3). These were

361   not associated with zones or quadrants, but were well recognizable, easy to grade

362   reproducibly for and may hold a hope to be implemented in the clinic. These

363   phenotypes were associated with vast areas of the peripheral retina, and were distinct

364   from macular changes. Their association with early or late AMD in the macula should

365   be investigated in follow-up studies. However, we do not yet know whether these

366   phenotypes are clinically relevant or not.

367   In summary, peripheral retina grading may be important for the fuller understanding of

368   the development and progression of AMD and potentially other diseases.[22] Whether

369   progression of peripheral abnormalities may be associated with the development or

370   progression of macular changes remains to be evaluated by follow-up studies. As

371   UWFI is becoming more widespread, we soon will be able to see whether peripheral

372   retinal changes influence the outcome of AMD and whether the results presented here

373   can be reproduced in other populations.

374

382

383 **<u>Figures legend</u>**

384 Figure 1. Representative images taken by the Optos P200CAF ultra-widefield laser

385 scanning ophthalmoscope: (A-C) false color images; (D-F) autofluorescent images.

386

387 Figure 2. Visual representation of detailed grading of peripheral retinal lesions in zones

388 4 and 5 broken down to quadrants in both right and left eyes. M=macula,

389 AF=autofluorescence, RPE=retinal pigment epithelium. The color scheme represents

390 the ranges of changes represented as the percent of all eyes. Values for crystalline

391 drusen, CNV and atrophy were very low and are only depicted in Supplementary Table

392 1 (available at http//aaojournal.org).

393

394

395 Figure 3. Representative images for the suggested new peripheral retinal phenotypes:

396 color images (A,C,E) and red free images (B,D,F). PHDF: Peripheral hard druse field;

397 PRD: Peripheral reticular degeneration; AD: Arcade drusen; PSDF: peripheral soft

398 drusen field.

399

400 Table 1. Basic characteristics of the 1,138 eyes phenotyped in the Reykjavik Eye Study

401 (percentages of totals are in brackets). A: changes on color images; B: autofluorescent

402 changes.

403

404 Table 2. Detailed macular and peripheral grading cross tabulation (percentages of

405 totals are in brackets).

406

407 Supplementary Table 1. Detailed grading of peripheral retinal lesions in zone 4 (Z4)

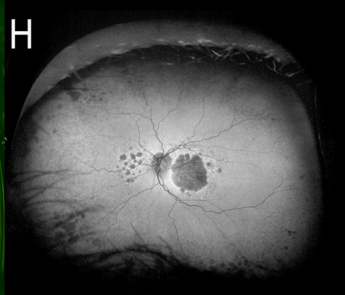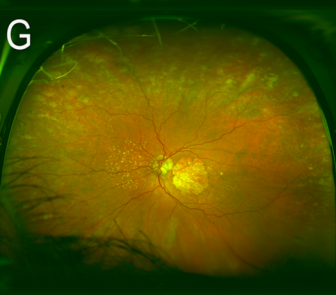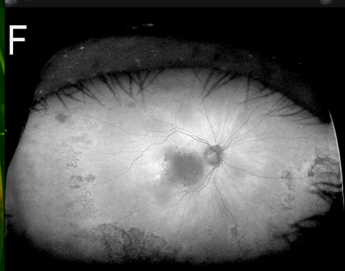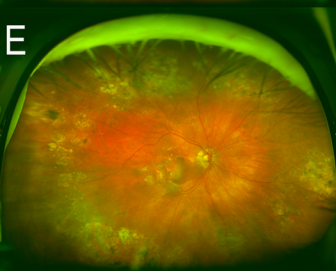408 and 5 (Z5) broken down to quadrants. SN=superior nasal; IN=inferior nasal;
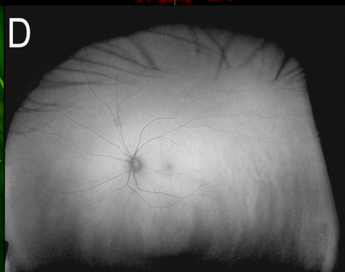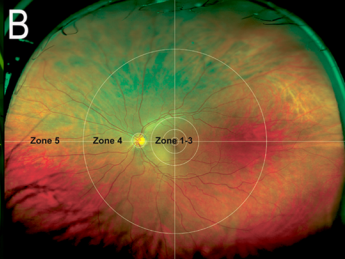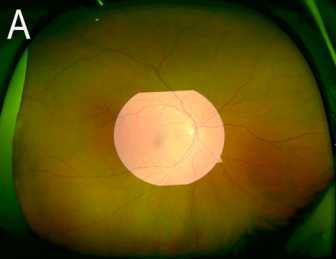
409   ST=superior temporal; IT=inferior temporal. Results are expressed as percent of all

410   eyes.

411

References

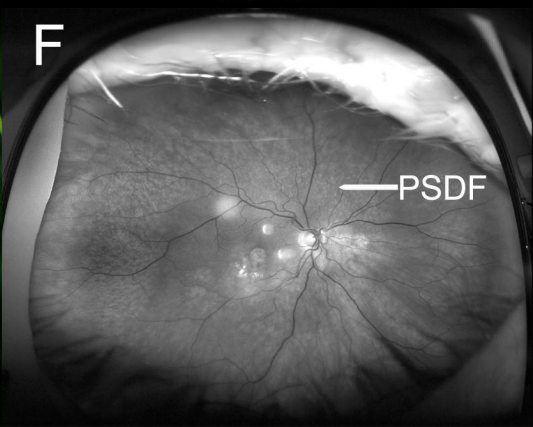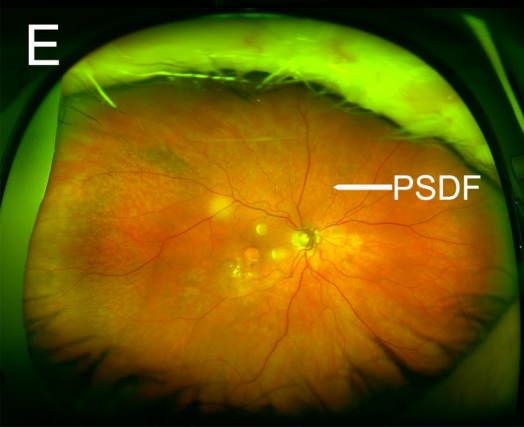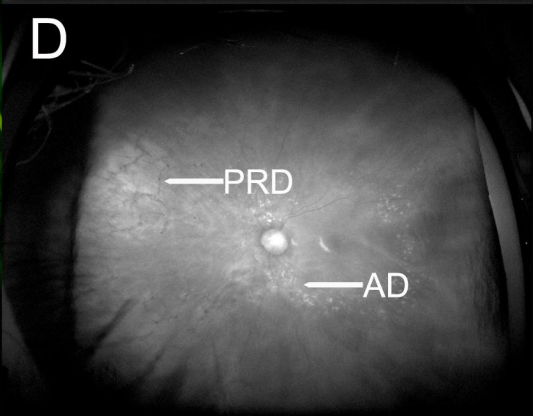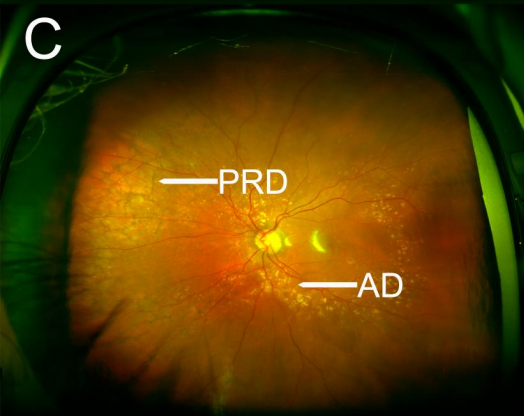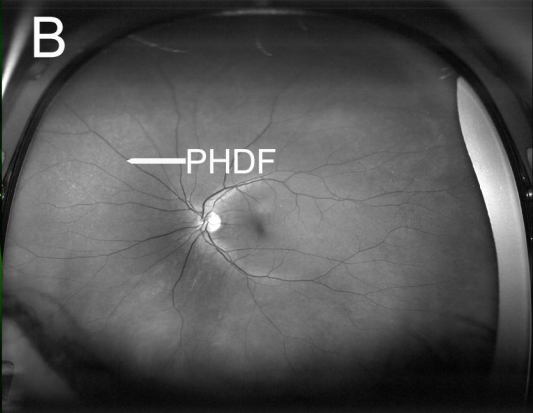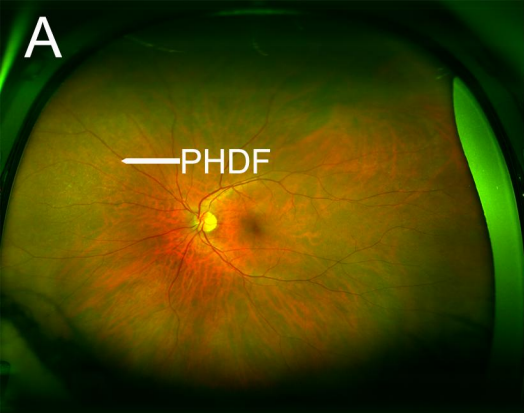[1] Bell, F. C., and Stenstrom, W. J. (1983) *Atlas of the peripheral retina*, Saunders, Philadelphia.

[2] Flinn, J. M., Kakalec, P., Tappero, R., Jones, B. F., and Lengyel, I. (2014) Correlations in Distribution and Concentration of Calcium, Copper and Iron with Zinc in Isolated Extracellular Deposits Associated with Age-Related Macular Degeneration, *Metallomics*.

[3] Chow, S. P., Aiello, L. M., Cavallerano, J. D., Katalinic, P., Hock, K., Tolson, A., Kirby, R., Bursell, S. E., and Aiello, L. P. (2006) Comparison of nonmydriatic digital retinal imaging versus dilated ophthalmic examination for nondiabetic eye disease in persons with diabetes, *Ophthalmology 113*, 833-840.

[4] Seddon, J. M., Reynolds, R., and Rosner, B. (2009) Peripheral retinal drusen and reticular pigment: association with CFHY402H and CFHrs1410996 genotypes in family and twin studies, *Investigative ophthalmology & visual science 50*, 586-591.

[5] Csutak, A., Lengyel, I., Jonasson, F., Leung, I., Geirsdottir, A., Xing, W., and Peto, T. (2010) Agreement between image grading of conventional (45 degrees) and ultra wide-angle (200 degrees) digital images in the macula in the Reykjavik eye study, *Eye (Lond) 24*, 1568-1575.

[6] Jonasson, F., Arnarsson, A., Sasaki, H., Peto, T., Sasaki, K., and Bird, A. C. (2003) The prevalence of age-related maculopathy in iceland: Reykjavik eye study, *Arch Ophthalmol 121*, 379-385.

[7] Bird, A. C., Bressler, N. M., Bressler, S. B., Chisholm, I. H., Coscas, G., Davis, M. D., de Jong, P. T., Klaver, C. C., Klein, B. E., Klein, R., and et al. (1995) An international classification and grading system for age-related maculopathy and age-related macular degeneration. The International ARM Epidemiological Study Group, *Survey of ophthalmology 39*, 367-374.

[8] (2001) The Age-Related Eye Disease Study system for classifying age-related macular degeneration from stereoscopic color fundus photographs: the Age-Related Eye Disease Study Report Number 6, *American journal of ophthalmology 132*, 668-681.

[9] Jonasson, F., Arnarsson, A., Peto, T., Sasaki, H., Sasaki, K., and Bird, A. C. (2005) 5-year incidence of age-related maculopathy in the Reykjavik Eye Study, *Ophthalmology 112*, 132-138.

[10] Landis, J. R., and Koch, G. G. (1977) The measurement of observer agreement for categorical data, *Biometrics 33*, 159-174.

[11] Lengyel, I., Tufail, A., Hosaini, H. A., Luthert, P., Bird, A. C., and Jeffery, G. (2004) Association of drusen deposition with choroidal intercapillary pillars in the aging human eye, *Invest Ophthalmol Vis Sci 45*, 2886-2892.

[12] Flinn, J. M., Kakalec, P., Tappero, R., Jones, B., and Lengyel, I. (2014) Correlations in distribution and concentration of calcium, copper and iron with zinc in isolated extracellular deposits associated with age-related macular degeneration, *Metallomics*.

[13] Kirkpatrick, J. N., Manivannan, A., Gupta, A. K., Hipwell, J., Forrester, J. V., and Sharp, P. F. (1995) Fundus imaging in patients with cataract: role for a variable

458   wavelength scanning laser ophthalmoscope, *The British journal of*
459   *ophthalmology 79*, 892-899.
460   [14] Neubauer, A. S., Yu, A., Haritoglou, C., and Ulbig, M. W. (2005) Peripheral retinal
461   changes in acute retinal necrosis imaged by ultra widefield scanning laser
462   ophthalmoscopy, *Acta Ophthalmol Scand 83*, 758-760.
463   [15] Neubauer, A. S., Kernt, M., Haritoglou, C., Priglinger, S. G., Kampik, A., and
464   Ulbig, M. W. (2008) Nonmydriatic screening for diabetic retinopathy by ultra-
465   widefield scanning laser ophthalmoscopy (Optomap), *Graefe's archive for*
466   *clinical and experimental ophthalmology = Albrecht von Graefes Archiv fur*
467   *klinische und experimentelle Ophthalmologie 246*, 229-235.
468   [16] Chou, B. (2003) Limitations of the Panoramic 200 Optomap, *Optom Vis Sci 80*,
469   671-672.
470   [17] Jones, W. L. (2004) Limitations of the Panoramic 200 Optomap, *Optom Vis Sci 81*,
471   165-166.
472   [18] Witmer, M. T., Parlitsis, G., Patel, S., and Kiss, S. (2013) Comparison of ultra-
473   widefield fluorescein angiography with the Heidelberg Spectralis((R))
474   noncontact ultra-widefield module versus the Optos((R)) Optomap((R)), *Clinical*
475   *ophthalmology 7*, 389-394.
476   [19] Wybar, K. C. (1954) Vascular anatomy of the choroid in relation to selective
477   localization of ocular disease, *The British journal of ophthalmology 38*, 513-517.
478   [20] Lutty, G., Bhutto, I., and McLeod, D. (2012) Anatomy of the Ocular Vasculatures,
479   In *Ocular Blood Flow* (Schmetterer, L., and Kiel, J., Eds.), pp 3-21, Springer
480   Berlin Heidelberg.
481   [21] Sasaki, H., Kawakami, Y., Ono, M., Jonasson, F., Shui, Y. B., Cheng, H. M.,
482   Robman, L., McCarty, C., Chew, S. J., and Sasaki, K. (2003) Localization of
483   cortical cataract in subjects of diverse races and latitude, *Investigative*
484   *ophthalmology & visual science 44*, 4210-4214.
485   [22] Ritchie, C. W., Peto, T., Barzegar-Befroei, N., Csutak, A., Ndhlovu, P., Wilson, D.,
486   Corridan, B., Goud, B., Cheesman, N., and Lengyel, I. (2011) Peripheral Retinal
487   Drusen as a Potential Surrogate Marker for Alzheimer's Dementia: A Pilot Study
488   Using Ultra-Wide Angle Imaging, *Invest. Ophthalmol. Vis. Sci. 52*, 6683-.
489

Zone 5   Zone 4   Zone 1-3

| | Right | Left |
| Temp | Nasal | Temp |

Hard drusen

Soft drusen

RPE change

Hypo AF

Hyper AF

M

■ >35%	■ 25-35%	■ 20-25%
■ 15-20%	■ 10-15%	□ 5-10%
□ <5%		
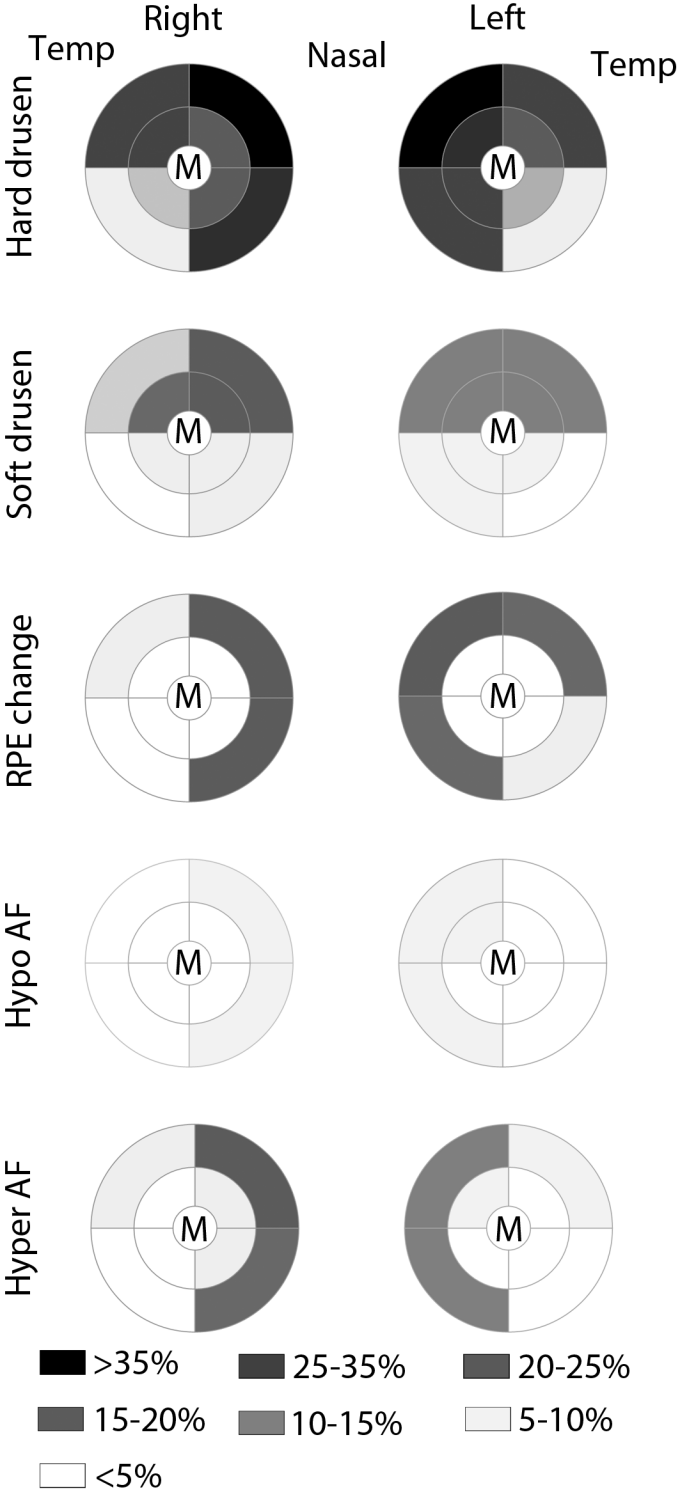
A		Periphery Color	
		Normal	Pathology
Macula Color	Normal	215 (18.9%)	115 (10.1%)
	Pathology	155 (13.6%)	653 (57.4%)

B		Periphery AF	
		Normal	Pathology
Macula AF	Normal	738 (67.7%)	202 (18.4%)
	Pathology	70 (6.4%)	81 (7.4%)

		Periphery				
		Normal	RPE Changes	Drusen only	Mixed	Atrophy
Macula	Normal	215 (18.9%)	9 (0.8%)	105 (9.2%)	0	1 (0.1%)
	Drusen only	154 (13.5%)	51 (4.5%)	560 (49.2%)	0	9 (0.8%)
	GA	0	0	8 (0.7%)	0	4 (0.4%)
	PED	0	0	2 (0.2%)	0	0
	CNV	0	0	11 (1.0%)	2 (0.2%)	0
	Mixed	1 (0.1%)	0	5 (0.4%)	0	1 (0.1%)

	RIGHT EYE					LEFT EYE		
ST	Z5	Z5	SN		SN	Z5	Z5	ST
	Z4	Z4				Z4	Z4	
	Z4	Z4				Z4	Z4	
IT	Z5	Z5	IN		IN	Z5	Z5	IT

Hard drusen

RIGHT EYE		LEFT EYE	
20.91%	40.72%	38.05%	23.43%
20.75%	17.61%	23.74%	18.24%
13.21%	17.77%	21.07%	13.05%
8.96%	25.63%	25.47%	10.06%

Soft drusen

RIGHT EYE		LEFT EYE	
9.43%	14.94%	13.99%	10.22%
10.53%	12.26%	14.31%	12.58%
6.45%	9.28%	7.39%	6.45%
3.62%	5.82%	5.82%	3.62%

Crystalline drusen

RIGHT EYE		LEFT EYE	
0.00%	0.16%	0.47%	0.00%
0.00%	0.31%	0.79%	0.31%
0.47%	0.16%	0.47%	0.31%
0.16%	0.16%	0.31%	0.00%

RPE changes

RIGHT EYE		LEFT EYE	
6.29%	17.61%	18.40%	10.53%
2.04%	2.20%	3.14%	2.36%
1.57%	1.73%	2.67%	1.73%
4.25%	15.09%	14.15%	7.39%

Hypo AF

RIGHT EYE		LEFT EYE	
1.73%	8.18%	7.08%	2.36%
2.67%	4.09%	5.97%	2.83%
2.99%	4.56%	4.09%	2.36%
1.73%	7.39%	5.35%	1.89%

Hyper AF

RIGHT EYE		LEFT EYE	
5.19%	16.04%	14.15%	6.76%
4.40%	7.08%	7.55%	4.25%
3.46%	6.29%	4.87%	3.46%
2.99%	11.95%	10.06%	4.25%

CNV

RIGHT EYE		LEFT EYE	
0.16%	0.00%	0.00%	0.16%
0.16%	0.00%	0.16%	0.79%
0.16%	0.00%	0.00%	0.63%
0.16%	0.00%	0.00%	0.00%

Atrophy

RIGHT EYE		LEFT EYE	
0.79%	0.63%	0.94%	0.94%
0.63%	0.31%	0.47%	0.63%
0.47%	0.16%	0.47%	0.31%
1.26%	0.94%	0.63%	0.94%